

SPACE CHARGE DRIVEN RESONANCES IN THE CERN PS

F. Asvesta^{*1,2}, H. Bartosik¹, A. Huschauer¹, Y. Papaphilippou¹
¹CERN, Geneva, Switzerland, ²NTUA, Athens, Greece

Abstract

In the CERN Proton Synchrotron space charge driven resonances are excited around the operational working point due to the periodicity of the optics functions. In this paper, the resonances are studied using analytical methods, i.e. the evaluation of the resonance driving terms connected to the space charge potential of Gaussian distributions. Furthermore, the resonances are characterized in measurements and simulations for various beams. The beams considered are different in terms of brightness, in order to study the dependence of the resonance strength on the space charge force.

INTRODUCTION

Space charge effects are critical for high-brightness synchrotrons such as the CERN Proton Synchrotron (PS). Space charge forces create an incoherent tune shift that depends on the longitudinal and transverse distributions, the energy and the intensity of the beam. This tune spread can be analytically estimated for Gaussian (transverse) beam distributions [1]. Figure 1 shows the expected space charge tune spreads for the beam parameters used during the experimental studies presented in this paper (summarized in Table 1).

The space charge potential can have an interplay with resonances through the space charge tune spread, but it can also directly excite resonances [2]. The Resonance Driving Terms (RDTs) of resonances driven by the space charge potential of Gaussian beams can be calculated analytically [2, 3]. In the PS an 8th order space charge driven resonance at $8Q_y = 50$ was identified in the past [4, 5]. Recent studies have confirmed the losses when crossing this resonance [6] and have identified another space charge driven resonance at $2Q_x + 6Q_y = 50$ [7].

In this paper, the 8th order space charge driven resonances in the PS are studied using the analytical expression for the respective RDTs. Moreover, experimental results of tune scans using the beams of Table 1 will be presented and complemented with simulation studies.

Table 1: Beam Parameters for Simulations and Experiments

Beam Type	High-brightn.	Low-brightn.
e_h^n (1 σ)[mm mrad]	5.5	5.5
e_v^n (1 σ) [mm mrad]	4.5	4.5
Intensity [10 ¹⁰ ppb]	96	48
$\Delta p/p_{rms}$ (1 σ)[10 ⁻³]	0.52	0.52
E_{kin} [GeV]	1.4	1.4

* foteini.asvesta@cern.ch

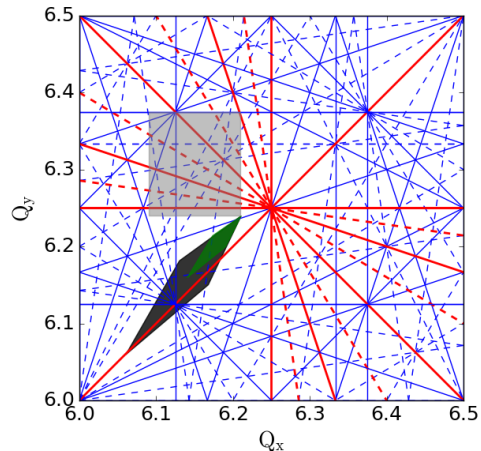


Figure 1: Sketch of the tune footprints for the beams of interest: high-brightness in black and low-brightness in green. Resonances of 3rd and 8th order are plotted, systematic in red and non-systematic in blue. The skew resonances are shown in dashed lines and the normal in solid. The grey shaded area corresponds to the tune space tested in the experimental studies.

ANALYTICAL CONSIDERATION

The excitation of resonances can be studied using perturbation theory on the non-linear Hamiltonian [8]. The leading order RDTs of the space charge driven resonances can be evaluated for the perturbing space charge potential of a Gaussian beam, given by [9],

$$V_{sc}(x, y) = \frac{r_0 N_B}{\beta^2 \gamma^3 \sqrt{2\pi} \sigma_s} \int_0^\infty \frac{-1 + \exp\left(-\frac{x^2}{2\sigma_x^2 + t} - \frac{y^2}{2\sigma_y^2 + t}\right)}{\sqrt{(2\sigma_x^2 + t)(2\sigma_y^2 + t)}} dt \quad (1)$$

where r_0 is the classical particle radius, N_B the bunch intensity, β, γ , the relativistic factors and $\sigma_{s,x,y}$ the longitudinal, horizontal and vertical beam sizes. A Python module for the calculation of the RDTs from the space charge potential of Gaussian beams has been developed [10] and is used to study the 8th order resonances in the PS, as discussed below.

The RDTs for the $8Q_y = 50$, $2Q_x + 6Q_y = 50$ and $4Q_x + 4Q_y = 50$ resonances have been evaluated for the high-brightness beam and are shown in Fig. 2. Note that the driving term values presented here are normalized by the distance from the resonance, i.e. $l - mQ_x - nQ_y$ where l, m, n the corresponding harmonic and order. The optics functions for the PS lattice, required for the calculation of the RDTs, have been obtained from MAD-X [11]. The 8th order driving terms for all of the resonances studied here increase significantly when the tune values are set on the

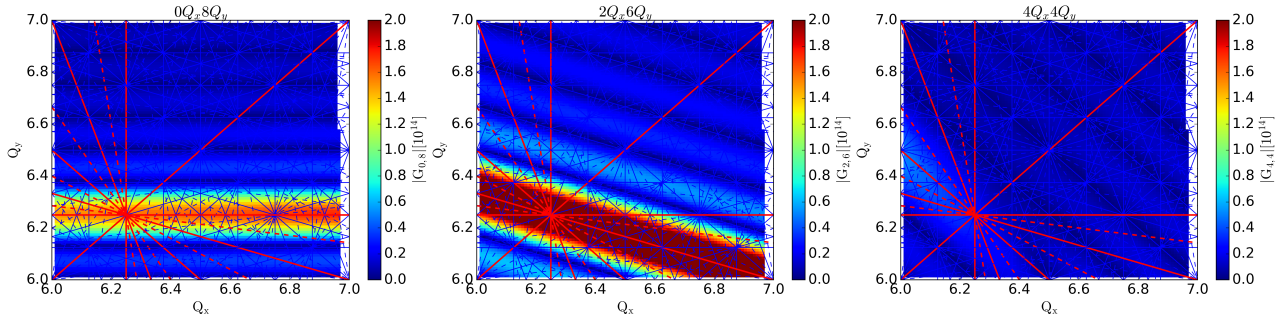


Figure 2: RDTs computed from the space charge potential of Gaussian distributions for the PS lattice for the $8Q_y$ (left), $2Q_x + 6Q_y$ (middle) and $4Q_x + 4Q_y$ (right) resonances. The color code corresponds to the amplitude of the respective driving term at each tune.

50^{th} harmonic, i.e. $8Q_y = 50$, $2Q_x + 6Q_y = 50$ and $4Q_x + 4Q_y = 50$. This harmonic coincides with the periodicity of the PS optics function modulation and consequently, the corresponding resonances are excited. On the other hand, the resonances at harmonics not present in the variation of the optics function of the lattice are not excited and the RDTs go to 0. It should be emphasized that the $8Q_y = 50$ and $2Q_x + 6Q_y = 50$ resonances appear much stronger than the $4Q_x + 4Q_y = 50$ resonance. Since the driving terms are computed directly from the space charge potential of Eq. 1, beams with different brightness will lead to different resonance excitation. In other words, the RDTs shown in Fig. 2 will be qualitatively the same but the amplitudes will depend on the beam brightness (intensity/emittance).

MEASUREMENTS

To study the effect of the space charge excited resonances in Fig 2, two different types of beams in terms of brightness, high-brightness and low-brightness, have been chosen. The beam parameters are shown in Table 1. In order to compare the behaviour of the two beams in terms of losses, the emittances and consequently the beam sizes were kept the same, while the intensity was changed to control the space charge potential. The associated space charge tune shifts are shown schematically in Fig. 1.

Several measurement campaigns were carried out using these two beams, with the aim of identifying the resonances based on beam loss. The PS lattice had to be kept as linear as possible in order to study the effect of the space charge driven resonances. Hence, linear coupling and the 3^{rd} order resonance at $3Q_y = 19$ were corrected [7]. A single bunch was always injected at the tune of interest and stored for 1.2 s in constant energy. The losses are measured using the intensity values at 15 ms and 1115 ms after injection. The static tune scans cover the tune space 6.24 to 6.37 in steps of $2 \cdot 10^{-2}$ in Q_x and 6.11 to 6.21 in steps of $5 \cdot 10^{-3}$ in Q_y for the high-brightness, while for the low-brightness the scan could be extended to lower tune values in Q_x , i.e. 6.09 to 6.21, while the vertical tunes studied were the same (see Fig. 1). The reason is that the beam with the smaller tune spread, $\Delta Q_x \approx \Delta Q_y \approx 0.08$, could be injected at $Q_x = 6.09$ while being unaffected by resonances at the integer tune of $Q_x = 6$.

The results of the measurements with the high-brightness and low-brightness beams are presented in Fig. 3.

The static tune scan with the high-brightness beam shows losses of $\approx 7\%$ along a line parallel to the 8^{th} order resonance at 6.25, Fig. 3 (top left). Likewise, losses of the same order appear on a line parallel to the coupled 8^{th} order resonance at $2Q_x + 6Q_y = 50$. The shift observed between the resonance line and the losses connected to it is in agreement to the space charge induced tune spread, as shown in Fig. 1. The maximum losses are observed for large horizontal tunes $Q_x > 6.18$ where the two resonances overlap and the bunch is affected by both of them at the same time. In addition, losses of similar amplitudes were observed from the 8^{th} order $4Q_x + 4Q_y = 50$, contrary to our expectations from the RDTs calculation. However, those losses could also be coming from some normal octupolar errors exciting the resonance in 4^{th} order, i.e. $2Q_x + 2Q_y = 25$.

The static tune scan with the low-brightness beam, Fig. 3 (top right), shows losses along parallel lines to the $8Q_y = 50$ and $2Q_x + 6Q_y = 50$. In this case the losses appear much closer to the respective resonances, due to the smaller space charge tune spread. Moreover, the losses are in the order of $\approx 3\%$ suggesting that the resonances are weaker when the space charge force is reduced. The resonance $4Q_x + 4Q_y = 50$ or $2Q_x + 2Q_y = 25$, appears to be enhanced indicating that the main contribution for the excitation is not the space charge force but some lattice non-linearity, exciting the resonance most likely in 4^{th} order as discussed above.

SIMULATIONS

The beams of Table 1 have been simulated including the space charge effect in PyORBIT [12]. The PS lattice is matched in MAD-X for the tunes tested in the experiments and is then tracked at constant energy to simulate the PS flat bottom. The PS model includes systematic higher order fields obtained by matching to the measured non-linear chromaticity [14]. Space charge is included in the simulations using a frozen model in which the kick is analytically calculated from the lattice functions, the intensity, the longitudinal and the transverse parameters of the beam using the Bassetti-Erskine formula [13]. The analytic solver allows simulating the beams using a small number of macroparticles, 3000 in

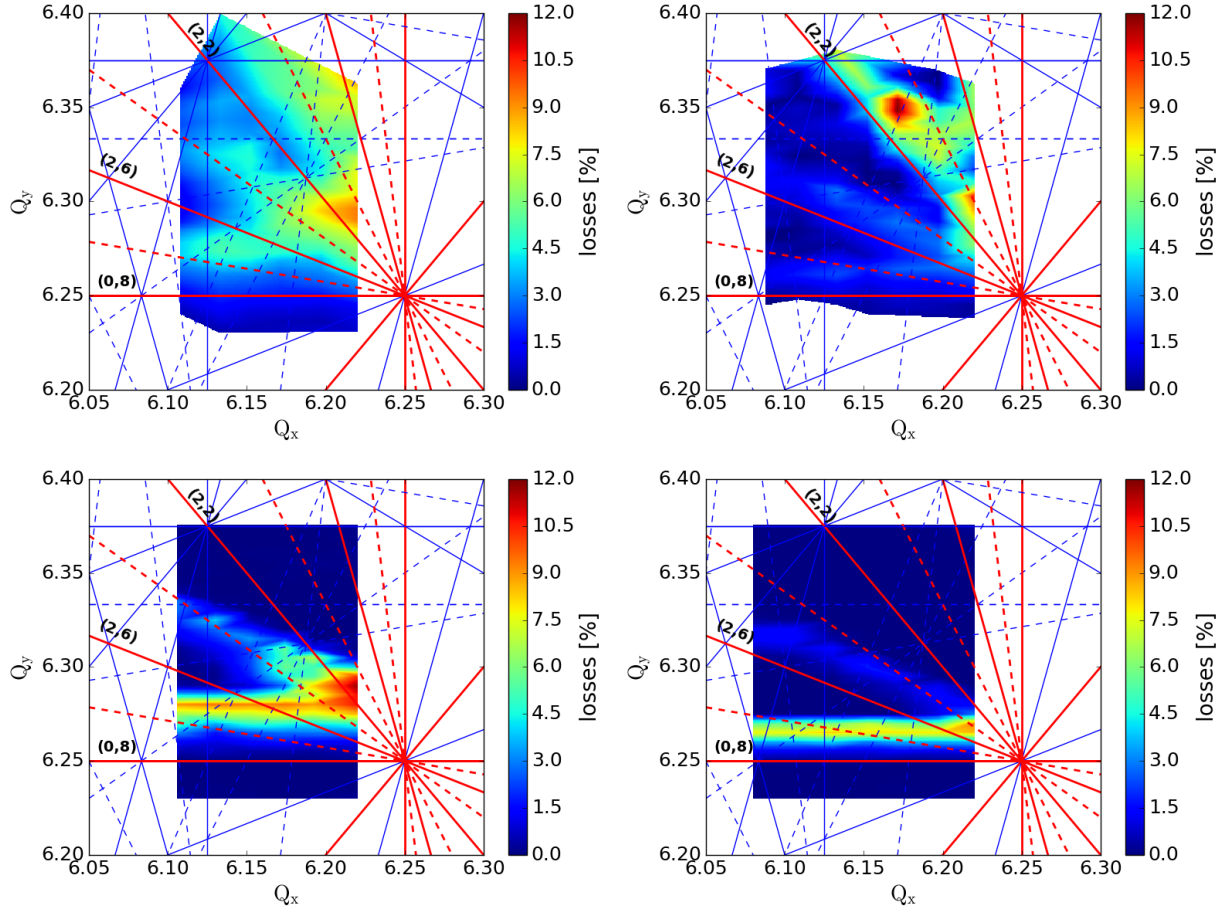


Figure 3: Measurements (top) and simulations (bottom) of the high-brightness (left) and low-brightness (right) beams. The color code represents losses after 1.1 s of beam storage. The order of the resonances observed is noted as (m, n) .

this case, making it possible to track for many turns. The equivalent tracking time to simulate the 1.2 s of storage in the PS, is $5 \cdot 10^6$ turns. The results of the simulations are shown in Fig. 3 (bottom) for both beams.

The simulations of the tune scan using the high-brightness beam agree well with the measurement results concerning the $2Q_x + 6Q_y = 50$ resonance. The resonance seems to get weaker and thinner as the tunes are moved far from $Q_x = 6.2$. Concerning the $8Q_y = 50$ resonance, simulations show slightly higher losses compared to measurements. Similar to the measurements, the losses are stronger when the resonances overlap. Regarding the $2Q_x + 2Q_y = 25$ resonance, no losses were observed in the simulations, further supporting the hypothesis that this resonance is driven by octupolar errors not included in our model. Furthermore, incomplete modelling of octupolar components in the machine could also be the origin of the difference between measurements and simulations concerning the resonance at $Q_y = 6.25$. On the other hand, the resonance $2Q_x + 6Q_y = 50$ would remain unaffected as in 4th order, it would be only excited in the presence of skew octupolar components.

In the simulations of the low-brightness beam the losses shown are concentrated at the $8Q_y = 50$ and $2Q_x + 6Q_y = 50$ space charge driven resonances, similar to the measurements.

The agreement between measurements and simulations concerning the $2Q_x + 6Q_y = 50$ resonance is satisfactory, while the discrepancy in the $Q_y = 6.25$ is slightly larger. The resonance $2Q_x + 2Q_y = 25$ is not observed in simulations. The fact that the discrepancy with the lower brightness beam is larger on the $Q_y = 6.25$ than the high-brightness supports the assumption of incomplete modelling of the normal octupolar components. Comparing the simulation results for both beams, there is a clear correlation between the strength of the resonances and the space charge.

CONCLUSION

In the CERN PS, resonances driven from space charge have been studied using analytic methods, measurements and simulations. Satisfactory agreement amongst the methods has been achieved. However, losses along the $2Q_x + 2Q_y = 25$ line observed only in measurements suggest that normal octupolar-like components may exist in the machine that are currently absent in the PS model.

ACKNOWLEDGEMENTS

The authors would like to thank F. Chapuis, the PSB and PS Operations teams and Prof. K. Hizanidis.

REFERENCES

- [1] K. Schindl, “Space Charge”, *CERN/PS 99-012(DI)*, 1999.
- [2] S. Machida, “Space-charge-induced resonances in a synchrotron”, *Nuclear Instruments and Methods in Physics Research Section A: Accelerators, Spectrometers, Detectors and Associated Equipment*, Volume 384, Issues 2–3, 1997.
- [3] S. Y. Lee, G. Franchetti, I. Hofmann, F. Wang and L. Yang, “Emittance growth mechanisms for space-charge dominated beams in fixed field alternating gradient and proton driver rings”, *New Journal of Physics*, Volume 8, Number 11, 2006.
- [4] S. Machida, “Space charge simulation for 4th order resonance”, *CERN Space Charge Collaboration Meeting*, Geneva, Switzerland, May, 2014, <https://indico.cern.ch/event/292362>.
- [5] R. Wasef *et al.*, “Space Charge effects and limitations in the CERN Proton Synchrotron”, *IPAC’13*, Shanghai, China, 2013.
- [6] F. Asvesta *et al.*, “Space charge studies in the PS”, *CERN Proceedings*, Volume 2, 2017, doi:10.23727/CERN-Proceedings-2017-002.37
- [7] F. Asvesta, H. Bartosik, A. Huschauer, Y. Papaphilippou and G. Sterbini, “Resonance identification studies at the CERN PS”, *Journal of Physics: Conference Series*, Volume 1067, 2018, doi:10.1088/1742-6596/1067/6/062021.
- [8] G. Guignard, “The general theory of all sum and difference resonances in a three-dimensional magnetic field in a synchrotron, pt 1”, *CERN-ISR-MA-75-23. ISR-MA-75-23*, 1975.
- [9] S. Kheifets, “Potential of a Three-Dimensional Gaussian Bunch”, Technical Report PETRA Note 119, 1976.
- [10] F. Asvesta *et al.*, “Resonance Driving Terms From Space Charge Potential”, Note to be published in CERN-ACC-NOTE-2019.
- [11] L. Deniau, E. Forest, H. Grote and F. Schmidt, “MAD-X User’s Guide”, <http://madx.web.cern.ch/madx/>, 2016.
- [12] PyORBIT Collaboration, “PyORBIT User’s Guide”, <https://github.com/PyORBIT-Collaboration/py-orbit>
- [13] M. Bassetti and G. A. Erskine, “Closed Expression for the Electrical Field of a Two-dimensional Gaussian Charge”, *CERN-ISR-TH/80-06*, 1980
- [14] A. Huschauer, M. Benedikt and R. Steerenberg, “Working point and resonance studies at the CERN Proton Synchrotron”, *CERN-THESIS-2012-212*, 2012